NJC

PAPER

View Article Online
View Journal

Cite this: DOI: 10.1039/c9nj00406h

A fluorescent sensor for thymine based on bis-BODIPY containing butanediamido bridges†

Jiahui Bi,[a] Xiaoyu Ji,[a] Meiyan Guo,[a] Hongyu Guo*[ab] and Fafu Yang *[abc]

Received 23rd January 2019,
Accepted 11th March 2019

DOI: 10.1039/c9nj00406h

rsc.li/njc

The sensor for thymine detection has a great significance in the analysis of deoxyribonucleic acid in living organisms. In this work, a series of bis-BODIPY derivatives, namely, **3a–3c** with diamido bridges were designed and prepared in yields of 74–77% through a simple procedure. The sensing abilities of compounds **3a–3c** for adenine, guanine, cytosine, thymine, glucose, urea and haemoglobin were examined by UV-vis and fluorescence spectra. Sample **3b** was demonstrated to be a good selective sensor for thymine among all the other tested species. The detection limit of sample **3b** was as low as 1.53×10^{-6} M for thymine. The competitive experiments suggested that the selective sensor for thymine was influenced slightly by the other species. The proposed sensing mechanism was confirmed by FT-IR, ^{1}H NMR and MS spectra. Sample **3b** exhibited good bioimaging performance with bright green fluorescence in living cell imaging. The significant fluorescence quenching phenomenon after the addition of thymine implied the sensing ability of sample **3b** for thymine in living cells.

Introduction

Deoxyribonucleic acid (DNA) is an important biomolecule in the living organisms, which encodes genetic information *via* four bases: guanine, adenine, thymine and cytosine.[1] The changes in the concentration of these bases may result in mutation or irregularity in the immune system and may also indicate the presence of various diseases such as intellectual disability, ageing, cancer, renal failure and cardiovascular diseases.[2] Therefore, the qualitative or quantitative analysis of these changes has a great significance.[3] Up to now, various analytical methodologies including gas chromatography,[4] liquid chromatography,[5] fluorescence spectroscopy,[6,7] immunocytochemical method,[8] capillary electrophoresis,[9] and electrochemical methods[10–14] have been used to determine the DNA bases in a variety of samples. Generally, most of these methods are expensive and tedious with complicated preparation processes for detecting materials and/or testing samples prior to instrumental analysis. Moreover, there are a few methods concerning the selective quantitative analysis of a special DNA base such as thymine from biological samples.[7] Hence, a simple and effective method for selectively detecting thymine or other DNA bases is expected.

In recent years, sensors based on fluorescence changes have attracted much attention due to their simple and efficient detection of ions or organic molecules. Among the numerous fluorophores, 4,4-difluoro-4-bora-3*a*,4*a*-diaza-*s*-indacene (abbreviated as BODIPY) and its derivatives have been considered as favourable fluorescent sensors due to their outstanding characteristics and photophysical properties including high excitation coefficients, high fluorescence efficiencies, high photostabilities, very low photo-toxicities, and negligible cytotoxicities.[15–21] As a result, many kinds of BODIPY derivatives were prepared by introducing various functional groups on the BODIPY skeletons, which exhibited effective fluorescence sensing abilities for metallic cations such as Hg^{2+},[22,23] Cu^{2+},[24,25] Zn^{2+},[26] Ag^{+},[27] Na^{+},[28] Cd^{2+},[29] and K^{+}.[30] Lately, some BODIPY-based fluorescent probes were also reported as effective sensors for organic functional species including polar biothiols,[31] formaldehyde,[32] and hydroxylamine.[33] Although much progress was made in the field of BODIPY-based sensors, no BODIPY-based fluorescent probes for thymine have been investigated so far. In this paper, a series of bis-BODIPY derivatives containing diamido bridges were designed and synthesized. The fluorescence sensing abilities of these novel BODIPY derivatives for DNA bases were investigated. The results suggested that the bis-BODIPY containing butanediamido bridges is a good selective sensor for thymine, which was observed for the first time for BODIPY probes. Moreover, it was applied successfully for the sensitive detection of thymine in living cells.

[a] *College of Chemistry and Materials, Fujian Normal University, Fuzhou 350007, P. R. China. E-mail: yangfafu@fjnu.edu.cn*
[b] *Fujian Key Laboratory of Polymer Materials, Fuzhou 350007, P. R. China*
[c] *Fujian Provincial Key Laboratory of Advanced Materials Oriented Chemical Engineering, Fuzhou 350007, P. R. China*

† Electronic supplementary information (ESI) available: Experimental details, supporting figures and table. See DOI: 10.1039/c9nj00406h

Results and discussion

Synthesis

The synthetic routes are illustrated in Scheme 1. According to previously reported procedures,[34] by treating diamines

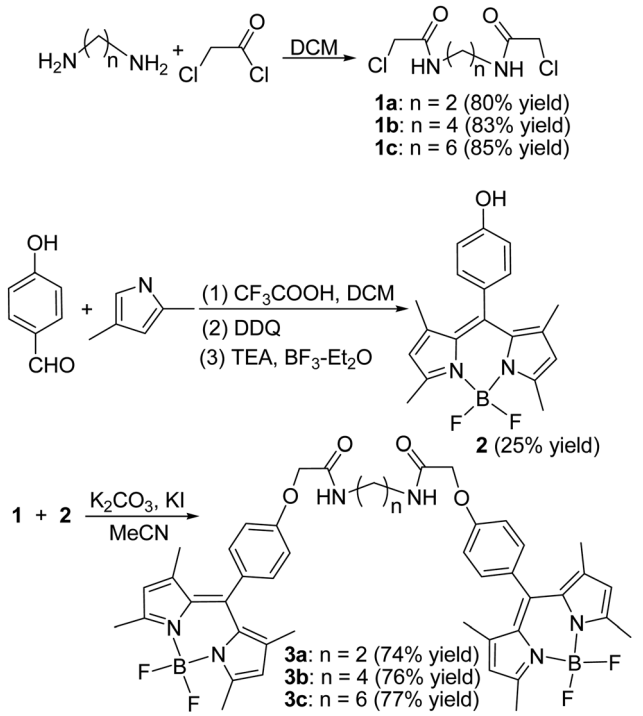

Scheme 1 The synthetic routes for target samples **3a**, **3b** and **3c**.

(ethylenediamine, butanediamine and hexamethylendiamine) with chloroacetic chloride, the corresponding chlorinated diamido derivatives **1a**, **1b** and **1c** were prepared conveniently. Also, using 4-hydroxy benzaldehyde and 2,4-dimethyl pyrrole as starting materials, OH-BODIPY **2** was obtained by sequential condensation, oxidation, and complexation reactions in the moderate yield of 25% after rapid columnar chromatography.[35] Finally, the target bis-BODIPY derivatives with diamido bridges **3a–3c** were synthesized *via* the "1+2" condensation of compounds **1a–1c** with compound **2** in the K_2CO_3/MeCN system using KI as a catalyst. The yields obtained after column chromatography were as high as 74–77%.

The structures of bis-BODIPY derivatives **3a–3c** were characterized by ^{1}H NMR spectra, ^{13}C NMR spectra, HR-ESI-MS spectra and elemental analysis (see ESI†). In ^{1}H NMR spectra, two singlets for CH_3, a pair of doublet and one singlet for ArH, one singlet for OCH_2CO and one broad singlet for NH certainly suggest that two BODIPY units are bridged by the diamido spacers. The data of ^{13}C NMR, HR-ESI-MS and elemental analysis were also in accordance with the structures of compounds **3a–3c**. It was worth noting that unlike the other reported bis-BODIPY structures,[30,36–42] compounds **3a–3c** are the first examples of bis-BODIPY derivatives bridged with soft diamido spacers, which is favorable to adjust the positional orientation of the two BODIPY units when binding guests in the cavities surrounded by BODIPY units and soft diamido spacers. Moreover, the amido (NH–C═O) groups also contributed to the binding of the DNA bases based on a strong hydrogen-bonding action. Thus, the sensing abilities of these novel bis-BODIPY derivatives for DNA bases were studied in detail.

Selective detection of thymine as a biochemical sensor

Biomolecules including adenine, guanine, cytosine, thymine, glucose, urea and haemoglobin were used for the selective detection of novel bis-BODIPY derivatives **3a**, **3b** and **3c**. The spectral changes in the UV-vis spectra and fluorescence spectra of samples **3a**, **3b** and **3c** with these biomolecules were investigated to determine their binding abilities. The UV-vis spectra are shown in Fig. S10–S12 (ESI†). It can be seen that the maximum absorbances of samples **3a**, **3b** and **3c** with different biomolecules fluctuate significantly (increase in varying degrees), indicating the strong interactions between samples **3a**, **3b** and **3c** and the tested species. Moreover, Fig. 1 illustrates the fluorescence spectra of samples **3a**, **3b** and **3c** with different biomolecules. One can see that all the maximum fluorescence emission wavelengths of samples **3a**, **3b** and **3c** exhibit no obvious changes (λ_{em} = 513 nm), indicating that the interactions between the samples **3a**, **3b** and **3c** and the tested species did not influence the conjugated molecular structures of BODIPY skeletons. Furthermore, the maximum emission intensities of these spectra exhibited remarkable changes, suggesting the existence of strong interactions between the samples **3a**, **3b** and **3c** and the tested species. As shown in Fig. 1A and C, compared to the fluorescence intensities of samples **3a** and **3c** with no tested biomolecules, the intensities of samples **3a** and **3c** with all the tested biomolecules decrease significantly. However, negligible binding selectivity was observed. The spectrum of sample **3b** with tested species exhibits different changes in comparison with those of samples **3a** and **3c**. The fluorescence intensities of sample **3b** with adenine, guanine, cytosine, glucose, urea and haemoglobin show slight decrease (decreasing ratio of 11–23%) from 540 to 433, 430, 440, 476 and 413, respectively. It was interesting that the fluorescence intensity of sample **3b** with thymine displayed outstanding decrease from 540 to 198 (decreasing ratio of 63%), indicating that it is an excellent selective sensor for thymine. The fluorescence quantum yields of sample **3b** in the absence of test species and in the presence of adenine, guanine, cytosine, glucose, urea, haemoglobin and thymine were measured as 0.93, 0.75, 0.73, 0.77, 0.83, 0.71, 0.86 and 0.33, respectively. These results also implied that sample **3b** possessed selective sensor abilities for thymine. Thus, the selective sensor abilities of sample **3b** for thymine were further studied in detail by fluorescence titration, ^{1}H NMR titration, binding ESI-MS spectra, binding FT-IR spectra, competitive experiments, and application in living cell imaging. The fluorescence quenching mechanism was also proposed and confirmed.

Fluorescence titration of thymine

A fluorescence titration of thymine was performed to explore the detecting behaviors of sample **3b** in detail. The fluorescence spectra of sample **3b** (1 μM) in DMSO/H_2O (1 : 9) solutions with different concentrations of thymine (1 μM) at λ_{ex} = 480 nm are shown in Fig. 2. By adding a series of different concentrations of thymine, the fluorescence could be quenched rapidly. For example, when we added 1.0 eq., 2.0 eq. and 5.0 eq. thymine to the solutions, the fluorescence intensities decreased to 37%,

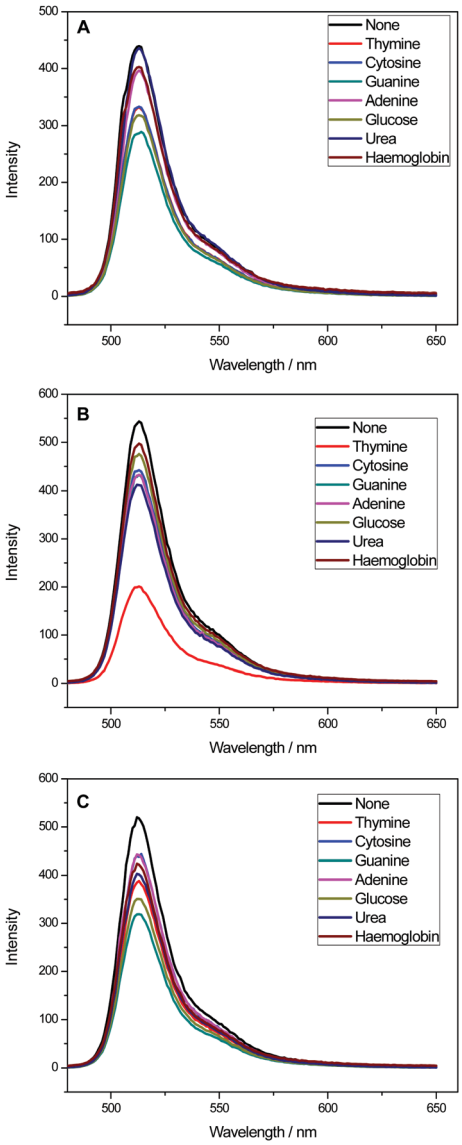

Fig. 1 Fluorescence spectra of samples **3a**, **3b** and **3c** (1 μM) in DMSO/H_2O (1 : 9) solutions with biomolecules (1 μM) at λ_{ex} = 480 nm. (A) Sample **3a**, (B) sample **3b**, and (C) sample **3c**.

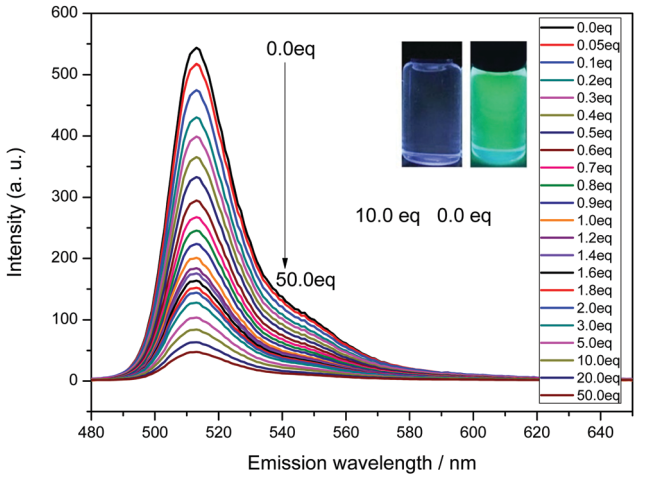

Fig. 2 Fluorescence spectra of sample **3b** (1 μM) in DMSO/H_2O (1 : 9) solutions with different concentrations of thymine (1 μM) at λ_{ex} = 480 nm. Inset: The fluorescence images of sample **3b** without and with thymine (5 μM), respectively.

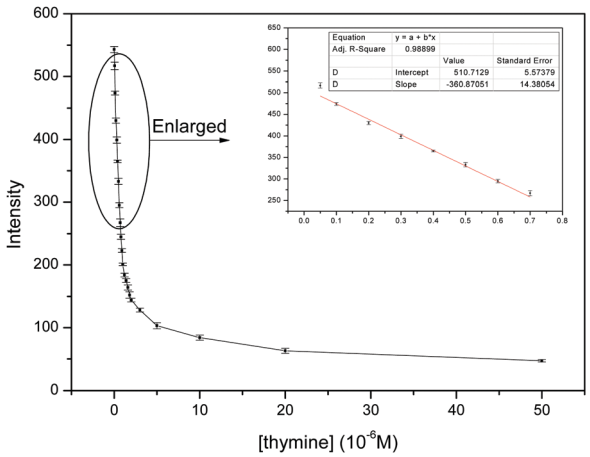

Fig. 3 Fluorescence intensity (513 nm) of sample **3b** (1 μM) in DMSO/H_2O (1 : 9) solutions with different concentrations of thymine (1 μM) at λ_{ex} = 480 nm. The inset shows the change in intensity from 0.05 to 0.7 μM concentrations of thymine.

26% and 19%, respectively. Furthermore, Fig. 3 illustrates the plot of fluorescence intensity at 513 nm *versus* the concentration of thymine. The plot between 0.05 eq. and 0.7 eq. of thymine is enlarged as the inset part, which shows a good linear relationship, thereby indicating the 1 : 1 binding stoichiometry for sample **3b** and thymine. Based on the calculated formula for the detection limit DL = $K \times$ Sb1/S (K = 2 or 3; taking the value = 2 here, Sb1 is the standard deviation of the blank solution and S is the value of the slope of the standard curve),[43] the detection limit could be calculated as DL = 1.53 $\times$ 10^{-6} M. This detection limit was low in comparison with the detection limits of thymine reported in literature,[7,13,14] suggesting that sample **3b** is a good sensor for thymine.

Interference experiments

The selective sensing of thymine by sample **3b** was further investigated by interference experiments with various biomolecules and metal cations. The results are shown in Fig. 4. One can see that the fluorescence intensities of sample **3b** with thymine fluctuate to a certain degree after the addition of interference species. The values of $(I_0 - I)/(I_0 - I_{thymine})$ changed in the range of 1.01–1.08, implying the slight influence of the interference species on selectively sensing thymine. These interference experiments suggested that sample **3b** is a good selective sensor for thymine under complicated circumstances containing other competing species.

pH influence on sensing abilities

The sensing stabilities in the pH range of 4–10 were investigated, as shown in Fig. 5. It can be seen that **3b** has good fluorescence stability at pH 6–8, and the fluorescence intensities decrease significantly when pH $<$ 6 or pH $>$ 8. Also, **3b** + thymine exhibited the strongest fluorescence quenching at pH = 7 and remained stable between pH 6 and 8. When pH $<$ 6 or pH $>$ 8,

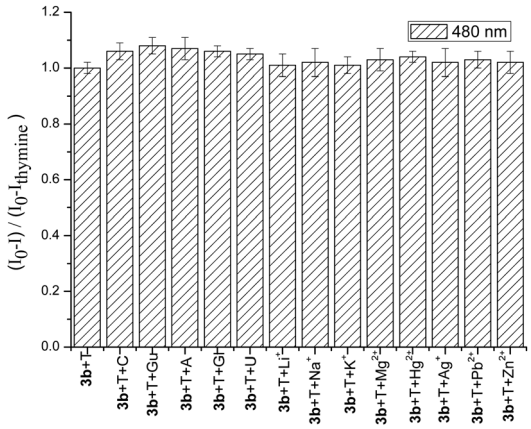

Fig. 4 Competitive experiments of sample **3b** + thymine with interfering species; [**3b**] = 1 μM, [thymine] = [interfering species] = 5 μM in DMSO/H_2O (1 : 9) solutions; λ_{ex} = 480 nm; T = thymine, C = cytosine, Gu = guanine, A = adenine, Gl = glucose, and U = urea.

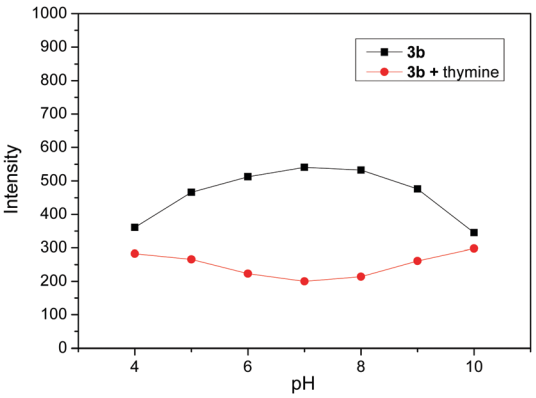

Fig. 5 The fluorescence intensities of **3b** and **3b** + thymine in DMSO/H_2O (1 : 9) solutions at different pH values; [**3b**] = [thymine] = 1 μM, λ_{ex} = 480 nm.

the fluorescence enhanced significantly, indicating that the sensing abilities became weak. These results implied that the pH values greatly influenced the sensing abilities and compound **3b** exhibited good sensing properties at pH 6–8 (the normal pH range of living bodies).

Detection mechanism

The detection mechanism for thymine was investigated *via* recording FT-IR spectra, ^{1}H NMR spectra and MS spectra. The FT-IR spectra of sample **3b** before and after binding thymine are displayed in Fig. 6. By comparing with the FT-IR spectra of sample **3b** and thymine, obvious changes were observed for the signals of H–NC═O and C–O bonds of sample **3b** with thymine. For example, the peak of H–NC═O in thymine and the C═O in sample **3b** at 3391 cm^{-1} and 1682 cm^{-1} shifted to 3210 cm^{-1} and 1727 cm^{-1}, respectively, indicating the existence of hydrogen bonds between sample **3b** and thymine. Furthermore, the comparison of the ^{1}H NMR spectra of sample **3b**, thymine and **3b** with thymine (1 : 1) is shown in Fig. 7. One can see that the signals of N–H for sample **3b** and thymine shift from a high field to a low field and the signals of OCH_2CO shift

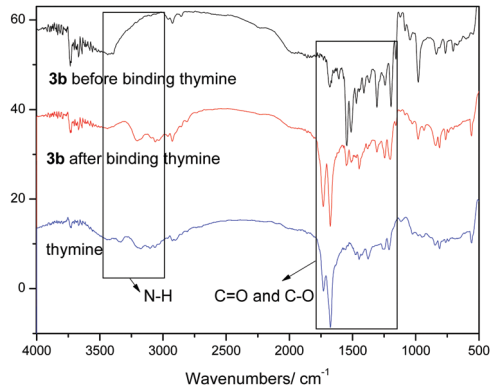

Fig. 6 FT-IR spectra of sample **3b** before and after binding thymine (1 : 1).

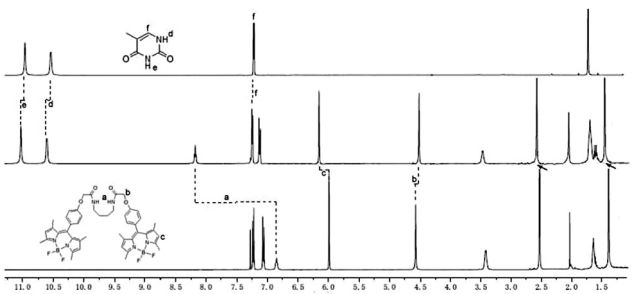

Fig. 7 The comparison of ^{1}H NMR spectra of sample **3b** (lower), thymine (upper) and **3b** with thymine (1 : 1) (middle).

from a low field to a high field, indicating the strong hydrogen-bonding action of N–H···O groups between the sample **3b** and thymine. The signals of ArH in the BODIPY skeleton shift from 5.97 ppm to 6.21 ppm and that of the methyl proton on BODIPY exhibits a down-field shift, suggesting the existence of π–π stacking between sample **3b** and thymine and the transfer of π-electron cloud from the BODIPY skeleton (π-donor) to thymine (π-receptor). Fig. 8 shows the ESI-MS spectra of sample **3b** with excess thymine (1 : 5). The results implied that only a 1 : 1 complex compound was observed at *m/z* of 975.7332. No other complex peak appeared even when excess thymine was added. This phenomenon suggested the presence of 1 : 1 binding system for sample **3b** with thymine, which was in accordance with the result of fluorescence titration. Thus, based on the results of FT-IR, ^{1}H NMR and MS spectra of sample **3b** with thymine, the possible binding model was proposed (Fig. 9). Before complexation, the alkyl group of the diamido bridge was in a random linear conformation, in which the distance between the two BODIPY units was too long to produce π–π stacking and the effect of the fluorescence quenching was very weak. However, after complexation with thymine, the distance between the two BODIPY units became less due to the hydrogen-bonding action between **3b** and thymine, resulting in enhanced π–π stacking of BODIPY–thymine–BODIPY, producing photoinduced electron transfer (PET) and finally strong fluorescence quenching. Due to π–π stacking, the aromatic ring plane of thymine was parallel to the BODIPY plane, due to which NH of thymine could not interact

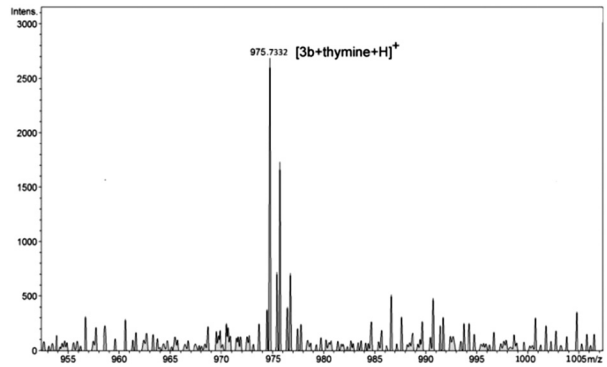

Fig. 8 The ESI-MS spectrum of sample **3b** with thymine (1 : 5).

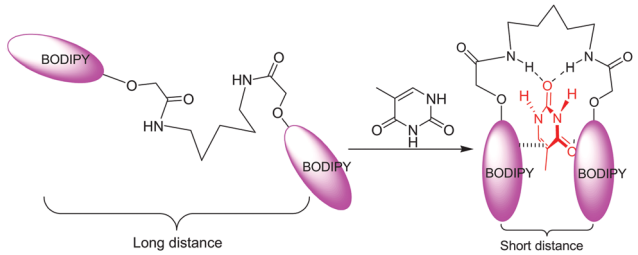

Fig. 9 The proposed binding mechanism of **3b** with thymine.

with **3b**, which agreed with the weak shift in the peak of NH of thymine after complexation. This proposed mechanism not only was in accordance with the results of the binding spectral studies but also explained well the fluorescence quenching in the fluorescence titration experiment. This kind of selective binding of thymine was observed for BODIPY derivatives for the first time.

Application in living cell imaging

As thymine is an important biomolecule in living organisms, it is interesting to investigate the thymine-sensing properties of sample **3b** in living cells, which are usually explored by fluorescence living cell imaging.[44–46] Therefore, the fluorescences in living cells with sample **3b** or sample **3b** and thymine were studied by confocal laser scanning microscopy (CLSM). On examining the MCF-7 cell metabolic activity with an MTT assay, it was found that the cell viability was above 89% under the concentration of 1.0 μM for 24 h at 37 °C (Fig. S13, ESI†). Then, by incubating with sample **3b** for 1 hour at 37 °C in a culture medium, MCF-7 cells were fixed. The fluorescence signals of living cells were detected at λ_{ex} = 488 nm. Fig. 10 illustrates the corresponding fluorescence images. These images suggest that the cells with sample **3b** exhibit bright green living cell images, indicating that the sample **3b** has excellent bioimaging performance. Moreover, after thymine was added in the culture medium, the brightness of fluorescence quenched obviously. These changes implied that sample **3b** is a good fluorescence sensor for thymine in living cells, and they were in accordance with the results of experiments in solution. These results confirmed the good bioimaging abilities of sample **3b** to sense thymine in living cells.

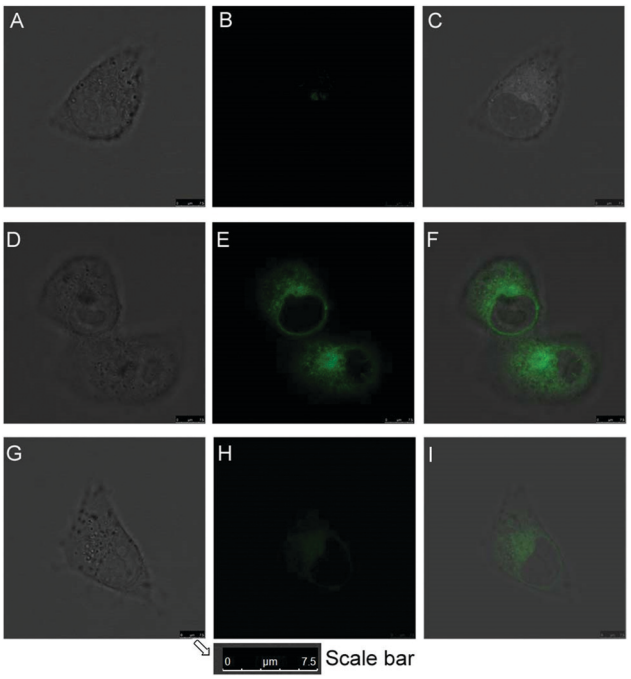

Fig. 10 Confocal fluorescence images of MCF-7 cells before and after incubation with sample **3b** (1.0 μM). (A)–(C) MCF-7 cells; (D)–(F) sample **3b**-MCF-7 cells; (G)–(I) sample **3b**-MCF-7 cells-thymine (5.0 μM). Left images are bright field images, middle images are fluorescence images, and right images are the merged images of fluorescence and bright field (λ_{ex} = 488 nm). Scale bar is the same for all the images (as shown in image G).

Conclusions

In conclusion, a series of bis-BODIPY derivatives **3a–3c** with diamido bridges were designed and synthesized in yields of 74–77%. The sensing abilities of compounds **3a–3c** for biomolecules including adenine, guanine, cytosine, thymine, glucose, urea and haemoglobin were investigated by UV-vis and fluorescence spectra. The results suggested that sample **3b** is a good selective sensor for thymine. The detection limit for thymine was as low as 1.53×10^{-6} M. The other species slightly influenced the selective sensing of thymine. The proposed sensing mechanism was supported by FT-IR spectra, ^{1}H NMR spectra and MS spectra. The experiment of living cell imaging of sample **3b** revealed that sample **3b** possessed good bioimaging performance with bright green fluorescence and exhibited sensing ability for thymine with the feature of fluorescence quenching, implying the application prospect in thymine detection in a living body.

Experimental

Chemicals and methods

All the chemical reagents were obtained from commercial suppliers and were used directly. TLC analysis was carried out on pre-coated glass plates. Column chromatography was performed using a silica gel (200–300 mesh). NMR spectra were recorded in $CDCl_3$ on a Bruker-ARX 400 instrument at 26 °C

using tetramethylsilane (TMS) as an internal standard. MS spectra were recorded using a Bruker mass spectrometer. Elemental analyses were performed using a Vario EL III Elemental Analyzer. The UV-vis spectra were measured on a Varian UV-vis spectrometer. Fluorescence spectra were recorded in a conventional quartz cell (10 × 10 × 45 nm) at 25 °C on a Hitachi F-4500 spectrometer equipped with a constant-temperature water bath and excitation and emission slits 10 nm wide. The fluorescence absolute quantum yield (Φ_F) was examined on an Edinburgh Instruments FLS920 Fluorescence Spectrometer with a 6-inch integrating sphere. Compounds **1a**, **1b** and **1c** were prepared according to previously reported methods.[33] Compound **2** was synthesized by a reported procedure.[29] The MCF-7 cancer cells were supplied by the School of Pharmacy, Fujian Medical University.

Synthetic procedure for compounds 3a, 3b and 3c

Under an N_2 atmosphere, a mixture of compound **1a** (**1b** or **1c**, 0.6 mmol), compound **2** (0.41 g, 1.2 mmol), dry K_2CO_3 (0.41 g, 3 mmol) and KI (0.10 g, 0.6 mmol) was stirred and refluxed in 30 mL of dry MeCN for 24 h. TLC detection suggested the disappearance of starting materials. After cooling, 50 mL of HCl solution (1 M) and 60 mL of CH_2Cl_2 were added to the reaction system. The obtained mixture was stirred for half an hour and then, the organic layer was separated. The organic portion was dried using anhydrous $MgSO_4$ and further concentrated under reduced pressure. The residue was purified by silica gel column chromatography (eluent: CH_2Cl_2 : petroleum ether = 4 : 1); bis-BODIPY derivatives **3a**, **3b** and **3c** were collected as red solids in yields of 74%, 76% and 77%, respectively.

Compound 3a. ^{1}H NMR (400 MHz, $CDCl_3$) δ (ppm): 1.37 (s, 12H, CH_3), 2.51 (s, 12H, CH_3), 3.55 (s, 4H, NCH_2), 4.55 (s, 4H, OCH_2), 5.95 (s, 4H, ArH), 7.05 (d, 4H, J = 8.0 Hz, ArH), 7.17 (d, 4H, J = 8.0 Hz, ArH), 7.43 (bs, 2H, NH); ^{13}C NMR (100 MHz, $CDCl_3$) δ (ppm): 14.34, 29.69, 39.80, 67.15, 115.20, 121.29, 128.42, 129.61, 131.66, 141.33, 142.80, 155.28, 157.68, 168.74; HR-MS (ESI) ($C_{44}H_{46}B_2F_4N_6O_4$) $[M + Na]^+$: calcd: 843.3809; found: 843.3829; anal. calcd for $C_{44}H_{46}B_2F_4N_6O_4$: C 64.41, H 5.65, N 10.24; found: C 64.45, H 5.59, N 10.18%.

Compound 3b. ^{1}H NMR (400 MHz, $CDCl_3$) δ (ppm): 1.39 (s, 12H, CH_3), 1.63 (s, 4H, CH_2), 2.54 (s, 12H, CH_3), 3.42 (s, 4H, NCH_2), 4.56(s, 4H, OCH_2), 5.97 (s, 4H, ArH), 6.83 (bs, 2H, NH), 7.04 (d, 4H, J = 8.0 Hz, ArH), 7.19 (d, 4H, J = 8.0 Hz, ArH); ^{13}C NMR (100 MHz, $CDCl_3$) δ (ppm): 15.06, 22.56, 29.52, 38.53, 67.16, 115.54, 121.02, 128.53, 129.65, 131.67, 141.08, 142.62, 155.39, 157.43, 167.91; HR-MS (ESI) ($C_{46}H_{50}B_2F_4N_6O_4$) $[M + Na]^+$: calcd: 871.4106; found: 871.4142; anal. calcd for $C_{46}H_{50}B_2F_4N_6O_4$: C 65.11, H 5.94, N 9.90; found: C 65.06, H 5.88, N 9.83%.

Compound 3c. ^{1}H NMR (400 MHz, $CDCl_3$) δ (ppm): 1.38 (s, 12H, CH_3), 1.57 (s, 4H, CH_2), 2.06 (s. 4H, CH_2), 2.52 (s, 12H, CH_3), 3.35 (bs, 4H, NCH_2), 4.52(s, 4H, OCH_2), 5.96 (s, 4H, ArH), 6.72 (bs, 2H, NH), 7.03 (d, 4H, J = 8.0 Hz, ArH), 7.20 (d, 4H, J = 8.0 Hz, ArH); ^{13}C NMR (100 MHz, $CDCl_3$) δ (ppm): 14.59, 23.30, 26.09, 29.39, 38.79, 67.28, 115.29, 121.29, 128.54, 129.64, 131.68, 141.06, 142.83, 155.51, 157.58, 167.48; HR-MS (ESI) ($C_{48}H_{54}B_2F_4N_6O_4$) $[M]^+$: calcd: 876.4979; found: 876.5011; anal. calcd for $C_{48}H_{54}B_2F_4N_6O_4$: C 65.77, H 6.21, N 9.59; found: C 65.71, H 6.17, N 9.51%.

MTT assay

Methylthiazolyldiphenyl-tetrazolium (MTT) trials were used to explore the toxicity for MCF-7 cancer cells. The inoculated MCF-7 cancer cells were cultivated at 37 °C and 5% CO_2 for 24 hours. Then, 1.0 μM of sample **3b** was tracked in the cells after incubating for 24 h. Furthermore, fostered cells were washed using PBS buffer and continued fostering for 3 hours in 0.5 mg mL^{-1} MTT–PBS buffer. Finally, 100 μL of DMSO was added to dissolve the generated formazan crystals, and the absorption intensity was examined at 490 nm.

The experiment of living cell imaging

Sample **3b** (3.0 mg) was dissolved in 1 mL of DMSO and then diluted using PBS buffer (pH = 7.4) to a concentration of 1.0 μM for imaging test. The MCF-7 cancer cells were cultivated in the same conditions as those used for MTT trials mentioned above for 24 h and then dyed by 1.0 μM of sample **3b**. After washing with PBS buffer, the dyed cells were treated to a solution of thymine (5.0 μM) for 1 hour at 37 °C. Then, the cells were imaged by a confocal laser scanning microscope (CLSM, Zeiss LSM 710, Jena, Germany).

Conflicts of interest

There are no conflicts to declare.

Acknowledgements

The financial support from the National Natural Science Foundation of China (no: 21406036), the Fujian Natural Science Foundation of China (no. 2017J01571), the Fujian Science and Technology Project (no. 2019N0010), the Fuzhou Science and Technology Project (2018-G-44) and the Undergraduate Innovation Program of FJNU (2018) are greatly acknowledged.

References

1 J. M. Berg, J. L. Tymoczko and L. Stryer, *Biochemistry*, WH Freeman and Company, 5th edn, 2002, pp. 118–119.
2 R. S. Sheng, F. Ni and T. M. Cotton, *Anal. Chem.*, 1991, **63**, 437–442.
3 Q. Xu and S. F. Wang, *Microchim. Acta*, 2005, **151**, 47–52.
4 D. P. Glavin, H. J. Cleaves, A. Buch, M. Schubert, A. Aubrey, J. L. Bada and P. R. Mahaffy, *Planet. Space Sci.*, 2006, **54**, 1584–1591.
5 A. M. de Carvalho, A. A. F. Carioca, R. M. Fisberg, L. Qi and D. M. Marchioni, *Nutrition*, 2016, **32**, 260–264.
6 S. Pang, Y. Zhang, C. Wu and S. Feng, *Sens. Actuators, B*, 2016, **222**, 857–863.
7 K. Shrivas, N. Nirmalkar, S. S. Thakur, R. Kurrey, D. Sinha and R. Shankar, *RSC Adv.*, 2018, **8**, 24328–24337.

8 A. A. Vink, R. J. Berg, F. R. de Gruijl, P. H. Lohman, L. Roza and R. A. Baan, *J. Invest. Dermatol.*, 1993, **100**, 795–799.
9 F. Q. Yang, L. Ge, J. W. H. Yong, S. N. Tan and S. P. J. Li, *J. Pharm. Biomed. Anal.*, 2009, **50**, 307–314.
10 A. Yari and S. Derki, *Sens. Actuators, B*, 2016, **227**, 456–466.
11 Y. S. Gao, J. K. Xu, L. M. Lu, L. P. Wu, K. X. Zhang, T. Nie, X. F. Zhu and Y. Wu, *Biosens. Bioelectron.*, 2014, **62**, 261–267.
12 P. Niedziałkowski, T. Ossowski, P. Zięba, A. Cirocka, P. Rochowski, S. J. Pogorzelski, J. Ryl, M. Sobaszek and R. J. Bogdanowicz, *J. Electroanal. Chem.*, 2015, **756**, 84–93.
13 K. L. Ng and S. M. Khor, *Anal. Chem.*, 2017, **89**, 10004–10012.
14 L. J. Feng, X. H. Zhang, P. Liu, H. Y. Xiong and S. F. Wang, *Anal. Biochem.*, 2011, **419**, 71–75.
15 X. T. Fang, H. Y. Guo, J. R. Lin and F. F. Yang, *Tetrahedron Lett.*, 2016, **57**, 4939–4943.
16 S. G. Awuah and Y. You, *RSC Adv.*, 2012, **2**, 11169–11183.
17 Y. Ni and J. Wu, *Org. Biomol. Chem.*, 2014, **12**, 3774–3791.
18 A. Kamkaew, S. H. Lim, H. B. Lee, L. V. L. Kiew, Y. Chung and K. Burgess, *Chem. Soc. Rev.*, 2013, **42**, 77–88.
19 W. Dehaen, V. Leen and N. Boens, *Chem. Soc. Rev.*, 2012, **41**, 1130–1172.
20 T. Kowada, H. Maeda and K. Kikuchi, *Chem. Soc. Rev.*, 2015, **44**, 4953–4973.
21 H. Lu, J. Mack, Y. Yang and Z. Shen, *Chem. Soc. Rev.*, 2014, **43**, 4778–4823.
22 M. J. Yuan, Y. L. Li and J. B. Li, *Org. Lett.*, 2007, **12**, 2313–2316.
23 B. X. Shen and Y. Qian, *Sens. Actuators, B*, 2017, **239**, 226–234.
24 A. B. More, S. Mula, S. Thakare, S. Chakrabory, A. K. Ray, N. Sekar and S. Chattopadhyay, *J. Lumin.*, 2017, **190**, 476–484.
25 Y. T. Chen, L. Y. Zhao and J. Z. Jiang, *Spectrochim. Acta, Part A*, 2017, **175**, 269–275.
26 A. N. Kursunlu and E. Guler, *J. Lumin.*, 2014, **145**, 608–614.
27 A. Coskun and E. U. Akkaya, *Tetrahedron Lett.*, 2004, **45**, 4947–4952.
28 K. Yamada, Y. Nomura, D. Citterio, N. Iwasawa and K. Suzuki, *J. Am. Chem. Soc.*, 2005, **127**, 6956–6959.
29 X. J. Peng, J. J. Du and J. L. Fan, *J. Am. Chem. Soc.*, 2007, **129**, 1500–1501.
30 Z. X. Yan, X. R. Lin, H. Y. Guo and F. F. Yang, *Tetrahedron Lett.*, 2017, **58**, 3064–3068.
31 D. Gong, Y. Tian, C. Yang, A. Iqbal, Z. Wang, W. Liu, W. Qin, X. Zhu and H. Guo, *Biosens. Bioelectron.*, 2016, **85**, 178–183.
32 T. Cao, D. Gong, S. C. Han, A. Iqbal, J. Qian, W. Liu, W. Qin and H. Guo, *Talanta*, 2018, **189**, 274–280.
33 A. C. Sedgwick, R. S. L. Chapman, J. E. Gardiner, L. R. Peacock, G. Kim, J. Yoon, S. D. Bull and T. D. James, *Chem. Commun.*, 2017, **53**, 10441–10444.
34 F. F. Yang, F. J. Yin, H. Y. Guo, Z. S. Huang and X. Y. Zhang, *J. Inclusion Phenom. Macrocyclic Chem.*, 2010, **67**, 49–54.
35 J. Y. Liu, H. S. Yeung, W. Xu, X. Li and D. P. K. Ng, *Org. Lett.*, 2008, **10**, 5421–5424.
36 S. Zrig, P. Rémy, B. Andrioletti, E. Rose, I. Asselberghs and K. Clays, *J. Org. Chem.*, 2008, **73**, 1563–1566.
37 A. Brown and M. R. Momeni, *J. Phys. Chem. A*, 2016, **120**, 2550–2560.
38 A. B. Nepomnyashchii, M. Bröring, J. Ahrens and A. J. Bard, *J. Am. Chem. Soc.*, 2011, **133**, 8633.
39 A. Wakamiya, T. Murakami and S. Yamaguchi, *Chem. Sci.*, 2013, **4**, 1002–1007.
40 H. Yokoi, S. Hiroto and H. Shinokubo, *Org. Lett.*, 2014, **16**, 3004–3007.
41 W. D. Pang, X. F. Zhang, J. Y. Zhou, C. J. Yu, E. H. Hao and L. J. Jiao, *Chem. Commun.*, 2012, **48**, 5437–5439.
42 Z. S. Li, Y. Chen, X. J. Lv and W. F. Fu, *New J. Chem.*, 2013, **37**, 3755.
43 M. Zhu, M. Yuan, X. Liu, J. Xu, J. Lv, C. Huang, H. Liu, Y. Li, S. Wang and D. Zhu, *Org. Lett.*, 2008, **10**, 1481–1484.
44 X. Zhang, K. Wang, M. Liu, X. Zhang, L. Tao, Y. Chen and Y. Wei, *Nanoscale*, 2015, **7**, 11486–11508.
45 Q. Cao, R. Jiang, M. Liu, Q. Wan, D. Xu, J. Tian, H. Huang, Y. Wen, X. Zhang and Y. Wei, *Mater. Sci. Eng., C*, 2017, **80**, 578–583.
46 R. Jiang, M. Liu, C. Li, Q. Huang, H. Huang, Q. Wan, Y. Wen, Q. Cao, X. Zhang and Y. Wei, *Mater. Sci. Eng., C*, 2017, **80**, 708–714.